Stimulated Desorption of Cations from Pristine and Acidic Low-Temperature Water Ice Surfaces

Janine Herring, Alex Aleksandrov, and Thomas M. Orlando*

School of Chemistry and Biochemistry and School of Physics, Georgia Institute of Technology, Atlanta, Georgia 30332, USA

(Received 21 November 2003; published 7 May 2004)

Electron-impact ionization of low-temperature water ice leads to H^+, H_2^+, and $H^+(H_2O)_{n=1-8}$ desorption. The 22 eV H^+ desorption threshold is correlated with localized 2-hole 1-electron and 2-hole final states which Coulomb explode, while the 22 eV H_2^+ threshold is due to H_2O^+ unimolecular dissociation. The 70 eV primary cluster ion threshold is consistent with holes in the $2a_1$ level and secondary ionization channels. All cation yields are sensitive to local structural changes and probe surface acidity. The cluster size distribution indicates hole-hole screening distances of 1–2 nm.

DOI: 10.1103/PhysRevLett.92.187602 PACS numbers: 79.20.Kz, 33.80.Rv, 34.80.Gs

The interaction of electrons with molecular solids is a topic of wide concern in astrophysics, materials physics, atmospheric physics, biophysics, planetary science, and environmental science. Of particular interest is the interaction of low-energy electrons with condensed water since this is important in (i) radiation processing of outer solar system grains and bodies [1], (ii) radiation damage of biological targets [2], (iii) formation of planetary atmospheres [3], and (iv) stimulating heterogeneous reactions possibly involved in loss of atmospheric ozone [4–7]. The electron-stimulated desorption (ESD) of energetic and thermalized neutral particles from ice can be explained in terms surface and self-trapped low-energy ($E < E_g$) exciton decay [8]. These excitons are also the parent states for 1-hole, 2-electron Feshbach resonances, which decay to yield primarily H^- [9,10] and O^- [9]. Because of the very local nature of the electron scattering resonances, H^- yields are dependent upon ice temperature and phase, and O^- yields are reduced due to the polarization interaction and lattice response.

The production and release of positively charged products from ice requires much more energy and is dominated by the desorption of protons with essentially no observable higher mass ions [11,12]. This is largely due to efficient hole hopping and delocalization brought about by the hydrogen bonding network [11,12] and the lattice response to local charges. In general, hole-localization probabilities and desorption of H^+, H_2^+, and $H^+(H_2O)_{n=1-8}$ should be very dependent upon the local hydrogen bonding network. Thus, ESD of H^+, H_2^+, and $H^+(H_2O)_{n=1-8}$ should be sensitive probes of the terminal ice structure and the dynamical interactions on ice surfaces.

In this Letter, we report the first electron-energy, phase, and temperature dependant ESD study of H^+, H_2^+, and $H^+(H_2O)_{n=1-8}$ from pristine and acidic ice surfaces. We present threshold energy measurements and a model for cluster formation involving competition between hole delocalization and Coulomb explosion. The yields of H^+, H_2^+, and $H^+(H_2O)_{n=1-8}$ change dramatically as a function of temperature or dangling bond density, ice phase, and HCl coverage. This is due to the geometric changes and increased hole localization associated with the disrupted hydrogen bonding network induced by increasing temperature and solvation of protons and Cl^-. The results also demonstrate that ESD is a sensitive probe of surface acidity.

The experiments were carried out in an ultrahigh vacuum (UHV) chamber (base pressure 2×10^{-10} Torr), equipped with a rotatable cryogenically cooled sample mount, time-of-flight (TOF) and quadrupole mass spectrometers (QMS), and a pulsed low-energy (5–250 eV) electron-beam. This supplies a time-averaged electron flux of about 6×10^{11} $e^-/cm^2\,sec^1$, in a spot size of roughly 0.5 mm^2. The low incident current precludes any beam-induced heating, gas-phase interactions, and surface charging [13]. The electron-beam incident angle was 45° with respect to the surface normal, and desorbing ions were collected using a TOF spectrometer mounted along the surface normal.

The UHV system was also equipped with two separate effusive dosing systems, and the samples studied were porous amorphous solid water (PASW) grown at 80 K, nonporous amorphous solid water (ASW) grown at 110 K, or crystalline ice (CI) grown at 140 K on either Pt(111) or oxidized zirconia substrates. All samples studied were >50 ML; this insured that interactions and variations in roughness associated with the underlying substrate were removed or minimized. Above ~90 K, the measured porosity is low and is similar for ASW and CI. PASW samples grown at 80 K have high porosities and apparent surface areas between 420 and 640 m^2/g [14]. Coverages were calibrated relative to the temperature programmed desorption (TPD) of water on Pt(111), and HCl doses were calibrated with the QMS and partial pressure changes. The surface temperature was monitored with a type-*K* thermocouple, and a computer-controlled

feedback drove the TPD and ESD ion yields versus temperature ramp.

Figure 1 shows the TOF distribution of cations produced and released from 50 ML of PASW deposited at 80 K [solid line, 1(a)] and CI deposited at 140 K [solid line, 1(b)] during 250 eV pulsed electron-beam bombardment. The TOF spectrum, which is dominated by H^+, shows a strong H_2^+ signal and a very reproducible $H^+(H_2O)_{n=1-8}$ distribution. The distributions observed are similar to those observed during the ESD of water nanoclusters adsorbed on rare gas overlayers [15], but differ from the previously reported distribution from ice [16]. Also shown in Fig. 1 (dotted lines) are TOF distributions obtained when the same samples have 0.06 ML of HCl. The changes are most significant for the CI case, with a large reduction in H^+ and H_2^+ and a significant increase in all cluster ion yields, especially the $H^+(H_2O)_{n=2}$ signal. Similar but less pronounced changes occur with PASW and ASW (not shown).

Before describing the mechanisms for ESD of H^+, H_2^+, and $H^+(H_2O)_{n=1-8}$ and the effects of substrate temperature, phase, and HCl ionization on these yields, we briefly review the electronic structure of water. The ground state of an isolated water molecule is $(1a_1)^2(2a_1)^2(1b_2)^2(3a_1)^2(b_1)^2$, where the $1a_1$ orbital is essentially the oxygen ($1s$) core level, the $2a_1$ and $1b_2$ orbitals are primarily involved in O-H bonding, and the $3a_1$ and $1b_1$ are primarily nonbonding. The two lowest

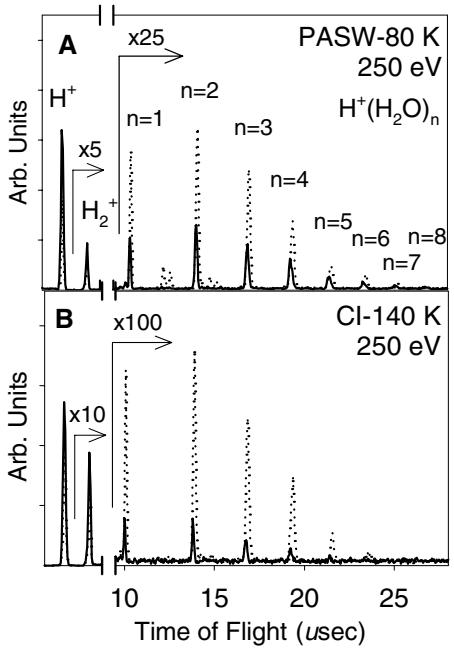

FIG. 1. The time-of-flight distribution of cations produced and desorbed during pulsed 250 eV electron beam irradiation of PASW (a) and CI (b). The solid lines represent data from pristine ice, whereas the dotted lines indicate the ion yield after addition of 0.06 ML of HCl. The HCl ionizes causing a large reduction in H^+ and H_2^+ and an increase in $H^+(H_2O)_n$ yields.

lying unoccupied orbitals are the $4a_1$ and $2b_2$. The $4a_1$ level is strongly antibonding and is mixed with the $3s$ Rydberg state. The electronic structure of ice is similar to that of gas-phase water; however, (i) the $2b_2$ orbital is replaced by a conduction band, (ii) the conduction band is very narrow and rather ill-defined, with a band minimum roughly 1 eV below the vacuum level, (iii) the valence levels are shifted slightly in energy, (iv) bands containing a_1 character have some dispersion, and (v) the $4a_1$ level, which is below the conduction band edge, is localized (excitonic) and maintains dissociative character.

The ESD threshold energy for H^+ and H_2^+ is ~ 22 eV, and a secondary H^+ threshold is near 40 eV. The $\sim$22 eV H^+ threshold is consistent with previous measurements [12,17] and has been assigned to configurationally mixed $(1b_1)^{-2}(4a_1)^1$ and $(3a_1)^{-1}(1b_1)^{-1}(4a_1)^1$ final states of water. It could also be associated with a $(2a_1)^{-1}$ direct dissociative ionization event [15]. The 40 eV threshold was associated with the $(3a_1)^{-2}(4a_1)^1$, $(3a_1)^{-1}(1b_2)^{-1}(4a_1)^1$, and $(1b_2)^{-2}(4a_1)^1$ states. Note all of the above mentioned 2-hole, 1-electron states can also have some $2b_2$ character, with the admixture dependent upon the local hydrogen bonding network and number of donor hydrogen bonds [18] at the surface. Though the $4a_1$ and $2b_2$ levels are dissociative, much of the dissociative force arises from Coulomb repulsions.

Some of the 2-hole states mentioned above can decay via *direct formation* of H_2^+. This complicated process has been reported in electron-impact studies of gas-phase water, albeit with a very low contribution ($\sim 2 \times 10^{-3}$) to the branching fraction observed in the dissociation of doubly ionized states of water [19]. A more recent study on multiphoton ionization and dissociation of water has revealed the presence of excited ion states that decay to form H_2^+ after absorption of four 532 nm photons by the initially produced water ions [20]. The final state energy was approximately 22 eV and the pathways for H_2^+ $(X^1\Sigma_g^+)$ formation was attributed to nonadiabatic dissociation via the X^2B_1 or excited B^2B_2 state of the water ion. These are the only doublet electronic states of H_2O^+ that have H_2^+ $(X^1\Sigma_g^+)$ as a dissociation product. We further note that the H_2^+ yield is linear with electron flux, consistent with unimolecular dissociation of states created during single impact events [21].

A weak threshold near 40 eV is observed for $H^+(H_2O)_{n=1-8}$ cluster ions; however, a more defined threshold is observable at $\sim$70 eV (see inset of Fig. 2). The threshold energy does not change with n, suggesting a similar mechanism for all clusters. Since this threshold energy is higher than the proton threshold, the states and formation mechanisms are probably different. Indeed, excitation energies > 70 eV produce the $(2a_1)^{-2}(1b_2)^2(3a_1)^2(b_1)^2$ state. The very local and repulsive hole-hole interaction in the $2a_1$ (bonding) level causes the formation of hot holes in the bulk and protons with > 7 eV kinetic energies at the surface. In addition, the 70 eV primary energy can also produce a $(2a_1)^{-1}$ hole

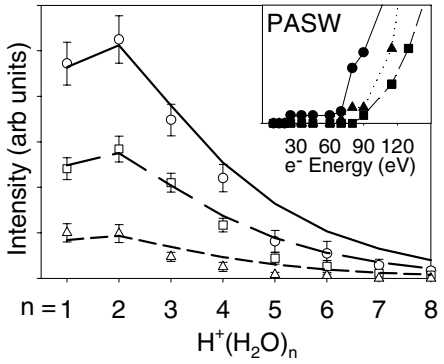

FIG. 2. Protonated cluster ion yield as a function of the number of water molecules (n). (○) is for PASW, (□) for ASW, and (△) for CI. The solid and dashed lines are empirical fits (see text). The inset shows the threshold energy for producing H_3O^+ (●), $H^+(H_2O)_2$ (▲), and $H^+(H_2O)_3$ (■). Similar thresholds were obtained for ASW and CI with lower yields.

and an energetic secondary electron which can produce another $(2a_1)^{-1}$ hole on a neighboring water molecule.

The interaction of a hole in a regular lattice site is energetically favorable and ultimately localizes to form a trapped proton in the form of a stable hydronium (H_3O^+) or dimer $H^+(H_2O)_2$ ion. Emission of $H^+(H_2O)_{n=1-8}$ is a statistical process that depends upon the energy required to break hydrogen bonds and overcome the potential induced by localized holes or trapped protons and the energy imparted by the potential field associated with the remaining localized charges. The data suggest that formation and desorption of cluster ion requires four steps: (i) efficient 2-hole localization primarily in the $2a_1$ level of water, (ii) hot hole transfer to the nearest-neighbor water molecule or hole formation in the $2a_1$ level of the nearest neighbor via a secondary ionization process, (iii) lattice polarization around the trapped charge forming a bonded $H^+(H_2O)_n$, and (iv) repulsion by the field of the second charged fragment (i.e., H^+, O^+, or OH^+). In the final step, the velocity of the desorbing ions is solely determined by the potential exerted by the localized charges and is independent of the mass. Indeed, our results, as well as previous work [22], show that the kinetic energy of the departing $H^+(H_2O)_n$ peaks at a few eV (not shown), and the distributions do not change with n.

Assuming these four steps, the intensity of a cluster with n water molecules can then be modeled with $I(n) \sim \exp\{-(E_H \times n + E_{sc}/n)/E\}$, where E_H is the energy of each hydrogen bond, n is the number of water molecules in the cluster, E_{sc} is the surface "core" level shift, and E is the effective cohesive energy. We have assumed an initial 2-hole separation distance of 3 Å, a screened surface core level shift of 0.7 eV [23], a 0.25 eV average hydrogen bond energy [24], and $E = 0.5$ eV. This formula is used to fit (solid and dashed lines) the observed experimental cluster ion distributions shown in Fig. 2. The largest yield is from PASW at 80 K (open circles) followed by ASW at 110 K (open squares), and CI at 140 K (open triangles). There are no structure specific parameters , and the fit is equally applicable for PASW, ASW, and CI.

The changes in the ESD ion yield with substrate temperature and phase are related to the mean roughness and thermally induced changes in the local hydrogen bonding network [11]. The data in the left portion of Fig. 3 demonstrate these strong effects. Specifically, the H^+ and H_2^+ yields increase strongly as a function of substrate temperature, and the onset of this is before any water sublimation. Surface water molecules containing dangling O-H bonds lead to proton formation, and the temperature dependence indicates increases in the number of dangling O-H bonds and excited state lifetimes [12]. Thus, the increased H^+ and H_2^+ yields can be associated with a reduction of hydrogen bonding in the near surface region, a reduction on the perturbation of the a_1 levels (particularly the mixed $3a_1$ and $4a_1$ levels), and an increased hole-localization probability in states containing significant a_1 character. The reduced hydrogen bonding interactions also lead to wave functions similar to that of the gas phase for the terminal water configurations via the return of atomic-p character in the $2b_2$ level [18].

However, the temperature dependence of the cluster ion signal is opposite of that observed for H^+ and H_2^+. This is important since the sublimation rate is increasing dramatically at the point where the cluster ion yield is at a minimum. Thus, gas-phase interactions are not playing a role in the production of cluster ions. The cluster ion threshold energy and the temperature dependence of the yields indicate that cluster ion formation and desorption requires a localized $2a_1^{-2}$ state or two $2a_1^{-1}$ holes in close

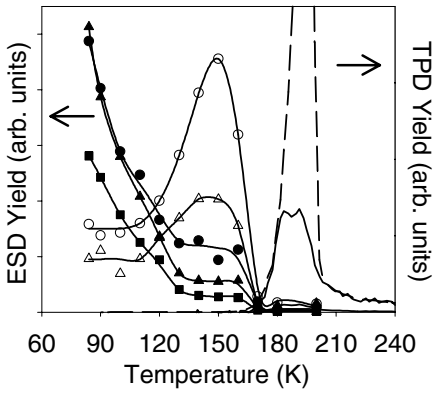

FIG. 3. Temperature dependence of electron stimulated cation yields (left axis) compared to thermal desorption data (right axis). The H^+ and H_2^+ yields are approximately a factor of 100 larger than the cluster ion yields. The H^+ (○) and H_2^+ (△) yields increase as a function of temperature, whereas the cluster ion yields [i.e., H_3O^+ (●), $H^+(H_2O)_2$ (▲), and $H^+(H_2O)_3$ (■)] decrease. These changes occur prior to any thermal desorption of H_2O (dashed line) and molecular HCl (solid line). Note the HCl and H_2O desorption processes are correlated.

proximity of one another. If these interactions occur directly on the surface, they will favor the production of H_3O^+ and cluster ions with a size distribution which can not exceed $n = 4$. Since we observe clusters up to $n = 8$, subsurface interactions and ledge-type defects are likely involved. The observed cluster size distribution also places a limit on the hole-hole screening distances, which is estimated to be ~1.0–2.0 nm.

As already shown in Fig. 1, the formation and desorption of H^+, H_2^+, and $H^+(H_2O)_{n=1-8}$ can be directly probed by dosing with HCl. The reconstruction and dynamic response of crystalline ice due to the interaction of HCl has been examined in recent quantum-mechanics/molecular-mechanics simulations [25]. More recent work on edge and surface defect sites using local density functional theory also predicts facile HCl ionization and strong lattice disruption due to ion-pair formation [26]. The facile ionization of HCl on low-temperature ice surfaces is supported by several experiments [27–29] and our observation of efficient H atom exchange from adsorbed HCl on D_2O ices and the commensurate thermal desorption of HCl with water. The TPD of 50 ML of D_2O (dotted line) containing 0.03 ML of HCl (solid line) is shown on the right side of Fig. 3. The TPD indicates that desorption of molecular HCl is correlated with the mobility and desorption of water. This correlated desorption *occurs only for doses of* HCl $\lesssim 0.5 \pm 0.2$ ML. We interpret this in terms of recombinative desorption of initially separated ion-pairs.

The important effect of preadsorbed ions can also be understood primarily in terms of reduced hydrogen bonding and perturbed dangling OH bonds accompanying ion-pair formation at the ice surface. The presence of protons leads to significantly altered water-water distances, and anions also distort terminal-OH bonds towards the local negative charge. These O-H bonds, which were the dominant proton ESD source, can no longer contribute to the proton yield as observed. At the temperatures used in these studies, anions are expected to remain on the surface and proton mobility may be limited as well [30]. If one assumes that the proton comes solely from surface defects, our observed yield at 90 K indicates an intrinsic CI surface defect density of $\sim 10^{12}$ cm^{-2}. Assuming $\sim 10^{15}$ sites/cm^{-2} for a hexagonal bilayer, this is 10^{-3} of the total surface sites available. The reduced proton signal and HCl coverage dependence implies HCl ionization involves multiple hexagons, subsurface lattice displacements, and possibly formation of domains, where $n > 6$.

In summary, we have examined low-energy electron-impact dissociative ionization of pristine and acidic low-temperature (<180 K) ice surfaces. H^+ desorption can be correlated with localized 2-hole 1-electron and 2-hole final states, which Coulomb explode, and H_2^+ desorption involves unimolecular decomposition of excited terminal H_2O^+. Cluster ions require 70 eV and involve hot holes in the $2a_1$ level and secondary ionization channels. When <0.5 ML of HCl interacts with the surface, the cluster ion yields increase dramatically whereas the H^+ and H_2^+ yields decrease. Cation ESD can be used to study local potential changes on low-temperature ice surfaces, providing one of the only experimental probes of surface acidity.

This work was supported by the U.S. Department of Energy, Office of Science, Contract No. DE-FG02-02ER15337.

*Corresponding author.
Electronic address: Thomas.Orlando@chemistry.gatech.edu

[1] M. T. Sieger, W. C. Simpson, and T. M. Orlando, Nature (London) **394**, 554 (1998).
[2] B. Boudaiffa *et al.*, Science **287**, 1658 (2000).
[3] R. E. Johnson, Rev. Mod. Phys. **68**, 305 (1996).
[4] Q. B. Lu and L. Sanche, Phys. Rev. Lett. **87**, 078501 (2001).
[5] M. A. Zondlo *et al.*, Annu. Rev. Phys. Chem. **51**, 473 (2000).
[6] M. Svanberg, J. B. C. Pettersson, and K. Bolton, J. Phys. Chem. A **104**, 5787 (2000).
[7] M. J. Molina *et al.*, Science **238**, 1253 (1987).
[8] G. A. Kimmel and T. M. Orlando, Phys. Rev. Lett. **75**, 2606 (1995).
[9] G. A. Kimmel and T. M. Orlando, Phys. Rev. Lett. **77**, 3983 (1996).
[10] W. C. Simpson *et al.*, Surf. Sci. **390**, 86 (1997).
[11] R. A. Rosenberg *et al.*, Phys. Rev. B **31**, 2634 (1985).
[12] M. T. Sieger, W. C. Simpson, and T. M. Orlando, Phys. Rev. B **56**, 4925 (1997).
[13] W. C. Simpson *et al.*, J. Chem. Phys. **108**, 5027 (1998).
[14] K. P. Stevenson *et al.*, Science **283**, 1505 (1999).
[15] R. Souda and J. Gunster, Phys. Rev. A **67**, 043201 (2003), and references therein.
[16] R. H. Prince and G. R. Floyd, Chem. Phys. Lett. **43**, 326 (1976).
[17] R. A. Rosenberg *et al.*, Chem. Phys. Lett. **80**, 488 (1981).
[18] M. Cavalleri *et al.*, Chem. Phys. Lett. **364**, 363 (2002).
[19] K. H. Tan *et al.*, Chem. Phys. **29**, 299 (1978).
[20] H. Rottke, C. Trump, and W. Sandner, J. Phys. B **31**, 1083 (1998).
[21] T. M. Orlando, A. B. Aleksandrov, and J. Herring, J. Phys. Chem. B **107**, 9370 (2003).
[22] R. Souda, J. Chem. Phys. **117**, 5967 (2002).
[23] K. Mase *et al.*, Surf. Sci. **451**, 143 (2000).
[24] E. D. Isaacs *et al.*, Phys. Rev. Lett. **82**, 600 (1999).
[25] Y. A. Mantz *et al.*, J. Phys. Chem. A **106**, 6972 (2002).
[26] K. Bolton, Theochem **632**, 145 (2003).
[27] F. Bournel *et al.*, Phys. Rev. B **65**, 201404 (2002).
[28] H. Kang *et al.*, J. Am. Chem. Soc. **122**, 9842 (2000).
[29] J. Harnett, S. Haq, and A. Hodgson, Surf. Sci. **532**, 478 (2003).
[30] J. P. Cowin *et al.*, Nature (London) **405** (1999).